Available online at www.sciencedirect.com
ScienceDirect
Ceramics International 37 (2011) 803–812
CERAMICS INTERNATIONAL
www.elsevier.com/locate/ceramint

Preparation and characterization of $CuFe_2O_4$ bulk catalysts

Julia E. Tasca [a], Claudia E. Quincoces [b], Araceli Lavat [a,*], Ana M. Alvarez [b], M. Gloria González [b]

[a] *Fac Ing. (UNCPBA), Av del Valle 5737, B7400JWI Olavarría, Argentina*
[b] *Centro de investigación Desarrollo en Ciencias Aplicadas Dr. J.J. Ronco (CINDECA) (CONICET-UNLP), 47 Nro 257, 1900 La Plata, Argentina*

Received 14 May 2010; received in revised form 9 August 2010; accepted 8 October 2010
Available online 19 November 2010

Abstract

This work is devoted to the investigation of the influence of the preparation process on the physical–chemical properties of a copper spinel applied as catalyst for hydrocarbon (HC) oxidation. Samples of $CuFe_2O_4$ mixed oxide belonging to the inverted spinel type structure have been obtained by high temperature solid state reaction and by wet chemical synthesis methods, applying nitrate and citrate precursor procedures, within the thermal range from 150 to 700 °C.

The bulk catalysts were characterized by XRD, TPR, FTIR, SEM-EDX, TEM and Mössbauer spectroscopy. Propane combustion was performed as a reaction test.

In this work it is demonstrated that the calcination temperature and chemical synthesis affect the crystal properties and cation distribution in the spinel structure, microstructure, surface area and reducibility; which are among the most relevant physical chemical properties for the catalytic activity. The materials obtained by wet chemical procedure, through nitrate and citrate routes, are better suited for propane combustion. This feature is assigned to the microstructure, to the presence of nanometric size particles and also to the cation distributions in the spinel sublattices of these materials.

Keywords: Cu–Fe spinel; Bulk catalyst; Synthesis; Characterization; Structure–properties correlation; Catalytic propane combustion

1. Introduction

The catalytic combustion of light alkanes, especially propane, is of great interest as a promising process for environmentally benign energy generation and emission control [1].

The most important advantages of this process are the low production of contaminant by products, i.e. NO_x, CO, etc. and the improvement of the energy efficiency.

A large number of metallic oxides belonging to different structural types, as spinels, perovskites, and K_2NiF_4, among others, have been reported for HC (hydrocarbon) combustion [2–4]. These groups of materials exhibit high electronic and oxygen ion conductivity, properties that are believed to be important for high activity in complete HC oxidation [5]. In addition to this, metallic oxides are less expensive and often thermally more stable than the noble metals, traditionally used for this purpose.

The ferrites with the formula MFe_2O_4, belonging to the spinel structural type, have received attention because of their unique properties and multiple applications in many fields, including ferrofluids, magnetic drug delivery and information storage [6].

Furthermore the catalysts based on ferrites $M^{II}Fe^{III}{}_2O_4$, (M = Cu, Co and Cr) are of great importance for catalytic processes, and particularly total oxidation of light HC [7,8]. The interaction between metallic cations results in the key factor for the catalytic process, mainly by preventing or inhibiting oxides sintering. Copper is one of the most used metals in several catalytic reactions. The distribution of Cu in the two different crystal sites in this structure is so far believed to keep the active sites separated, prolonging the activity and stability of catalysts [9].

Due to the practical reasons mentioned above, magnetic ferrite particles must have the reduced size and uniform shape and therefore improved synthetic procedures are required. Therefore, various preparation routes, microstructure and physical–chemical properties of copper ferrite have been reported in many papers [10].

* Corresponding author. Tel.: +54 02284 451055; fax: +54 02284 451055.
E-mail address: alavat@fio.unicen.edu.ar (A. Lavat).

0272-8842/$36.00
doi:10.1016/j.ceramint.2010.10.023

Nevertheless, the correlation between the catalytic behavior with the structure and the preparation procedure has been scarcely discussed.

The aim of this work is to report the effect of the synthetic procedure, the temperature of activation and the structural features on the catalytic activity of bulk $CuFe_2O_4$, obtained by different synthetic procedures. The materials were characterized by XRD, FTIR, TPR, SEM-EDX and Mössbauer spectroscopy. In order to study the correlation between the structural properties and the reactivity of the solids, the propane oxidation in a fixed bed reactor at atmospheric pressure and programmed temperature as reaction test was carried out. High temperature and mild preparation methods were used in order to evaluate the influence of the physical–chemical properties on the catalytic activity depending on the synthesis route.

2. Experimental part

2.1. Catalyst preparation

Three types of $CuFe_2O_4$ samples were prepared by different solid state and wet-chemical synthesis methods, i.e. *Solid phase synthesis* (*SP*), *Synthesis from nitrate precursors* (*NIT*) *and Citric acid-aided process* (*CIT*). The detailed synthetic procedures are described below.

2.1.1. Solid phase synthesis (SP)

A polycrystalline sample of bulk copper ferrite was prepared by conventional solid state reaction, by firing intimate stoichiometric mixtures of CuO and Fe_2O_3 (p.a. Riedel-de Haën). Reactions were carried out in air, in platinum crucibles, at 950 °C. The sample was maintained at this temperature, in the furnace, during 8 h. Heating was interrupted several times to grind the reaction mixture to facilitate the reaction progress.

A slow cooling down to room temperature leads to a tetragonally distorted spinel structure. In order to retain the high temperature cubic spinel structure, the sample was cooled to around 760 °C in the furnace and then quenched to room temperature in air [11].

2.1.2. Synthesis from nitrate precursors (NIT)

This synthetic procedure was employed to prepare copper ferrite from solution residues in order to facilitate the mixing of the oxides before calcination. Appropriate stoichiometric quantities of $Cu(NO_3)_2{\cdot}3H_2O$ (Riedel-de Haën) and $Fe(NO_3)_3{\cdot}9H_2O$ (Malinckrodt) in order to make 3 g product were added to 50 ml of distilled water and the resulting solution was heated to dryness, over a magnetic plate at 95 °C. The resulting brown solid was treated at 150 °C to allow the complete decomposition of nitrates and then calcined in a furnace at 700 °C, during 8 h. The powder was removed from the furnace and reground in a mortar five separate times to facilitate the reaction.

2.1.3. Citric acid-aided process (CIT)

This chemical synthesis involves both metals in a complex formation. Aqueous solutions of the individual nitrates were prepared and then mixed with aqueous citric acid into 50 ml of a homogenous solution. One equivalent mole of citric acid was applied to each total equivalent mole of the metals, in order to obtain the chelate complex. The aqueous solution was then concentrated by heating with vigorous stirring until viscous brown slurry was obtained at 70 °C. This slurry was dehydrated at about 80 °C in a sand bath for 2 h and the product was finally dried under vacuum in an oven at 95 °C. During this thermal treatment the volume of the gel increases markedly showing big pores and a puffy appearance. After grinding in a mortar, the fine powder was subjected to the following thermal schedule: 4 h at 150 °C, 4 h at 400 °C and 4 h at 700 °C, with intermediate millings. Samples were taken from the furnace after the thermal treatment at each one of the mentioned temperatures, in order to study the thermal decomposition of the precursor.

Wet chemical methods allowed obtaining the spinel phase at lower a temperature than the traditional ceramic method. At the same time, it was possible to achieve a powder with greater homogeneity and smaller size particles, since departing from the aqueous solutions allows the atomic mixing of elements involved in the mixed oxide formation.

2.2. Catalysts characterization

The samples were characterized by X-ray diffraction (XRD), Fourier transform infrared spectroscopy (FTIR), Thermo gravimetric and differential thermal analysis (TGA/DTA), Mössbauer spectroscopy (MS), electron microscopy (SEM, TEM), Textural parameters by BET and temperature programmed reduction (TPR).

A Philips PW 3710 diffractometer, with copper anode and graphite monochromated Cu Kα radiation was used. The unit cell parameters were obtained by a minimum squared procedure and refined with a locally modified version of the Werner PIRUM programme.

The FTIR spectra were measured using a Magna 550, Nicolet instrument equipped with CsI optics using the KBr pellets technique.

TGA/DTA experiments were carried out on the supported catalysts, using a Shimadzu TGA-50 instrument. The catalysts were submitted to a heat treatment (10 °C min^{-1} up 700 °C) in an air flow of 40 cm^3 min^{-1}.

The Mössbauer spectra were obtained in transmission geometry with a 512-channel constant acceleration spectrometer, at room temperature (RT). A source of ^{57}Co in Rh matrix of nominal 50 mCi was used. Velocity calibration was performed against a 12 μm-thick α-Fe foil. All isomer shifts (δ) mentioned in this paper referred to this standard. The Mössbauer spectra were evaluated using a commercial fitting program named Recoil, assuming Lorentzian lines. The spectra were folded to minimize geometric effects.

The solid morphologies were analyzed in a Philips, model SEM 550 with EDAX analyzer. An Au film was deposited on the samples to achieve a good resolution in the obtained images.

The mean particles sizes were estimated from the TEM photographs according to a mean surface diameter, [12]. The

TEM observations were carried out on a JEOL 100CX microscopy.

Textural parameters, specific surface and pore volume were determined by nitrogen adsorption at 77 K, in an Accusorb 2100E Micrometrics equipment. Data were interpreted using the BET equation.

Activity tests were carried out in a fixed bed micro reactor at atmospheric pressure and at temperature range from 200 °C to total conversion. The quartz tube reactor (10 mm i.d.) containing 0.120 g. catalyst was placed inside a tubular electrical furnace. The temperature was monitored by a cromel–alumel thermocouple placed in contact with the surface of catalyst bed. The usual temperature ramp was 1 °C min^{-1} and the gas flow rate was 100 cm^3 min^{-1}. The feed gas contains 1000 ppm C_3H_8, 1000 ppm NO, 4% O_2 and He as balance. The feed and effluent mixture gas was analyzed by an on-line Shimadzu GC-8A chromatograph with thermal conductivity detector (TCD) using a CTR1 column (Alltech), and He as carrier gas (20 cm^3 min^{-1}). N_2 and NO_2 were never detected in the effluent. Propane combustion was studied by determining the hydrocarbon conversion as a function of temperature (light-off curves).

3. Results and discussion

3.1. DRX characterization

The crystal lattice of the stable low-temperature phase of $CuFe_2O_4$ exhibit a tetragonal distortion, mainly due to the Jahn–Teller effect of Cu(II) cations, and above 760 °C is cubic [11]. Tetragonal $CuFe_2O_4$ is an inverse spinel in which Cu(II) cations occupy mainly octahedral B-sites, whereas Fe(III) cations are found on B-sites and tetrahedral A-sites with approximate equal occupancy [13]. The metastable cubic phase can be obtained by rapid quenching from high temperature, around 900 °C, to room temperature. It has been established, for Jahn–Teller distortion of the copper ferrospinel, that a critical number of octahedral site Cu(II) is ca 0.8 ions per formula unit for a cooperative distortion to tetragonal symmetry at RT [14].

XRD analysis of bulk catalysts demonstrated the presence of cubic spinel as single phase in the catalysts prepared by SP method, whereas those obtained, at lower temperature from the nitrate and citrate routes, displayed a tetragonal spinel structure in accordance with the previous reports [15,16].

The XRD patterns of the catalyst prepared by SP were measured during heating. After the thermal treatment at 700 °C the sample contains Cu and Fe_2O_3 but no copper ferrite was formed. The characteristic peaks of $CuFe_2O_4$ are observable at 800 °C, although the main components are still CuO and Fe_2O_3. The catalyst sample had to be calcined over 900 °C, in order to obtain pure copper ferrite, suggesting that by this route; it is only possible to synthesize this material at high temperature. Further sintering up to 950 °C helps to increase peak intensities and crystallinity. The XRD pattern of the sample SP950, shown in Fig. 1, was indexed to a single of cubic $CuFe_2O_4$ spinel and a refined unit cell parameter of 8.356(8) Å, in coincidence with JCPDF file No. 25-0583.

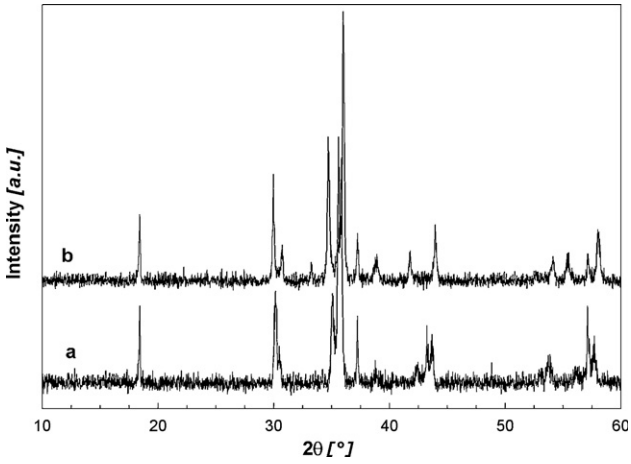

Fig. 1. XRD patterns: (a) SP950 and (b) NIT700.

In the case of the sample prepared at a lower temperature, around 700 °C by the nitrate route, i.e. NIT700, the diffractogram, also shown in Fig. 1, clearly confirms the presence of tetragonal $CuFe_2O_4$ spinel (JCPDF No. 06-0545). This pattern was indexed and the calculated cell parameters were a: 8.234(1) Å and c: 8.646(3) Å, with c/a: 1.05, in accordance with the reported values [15].

The evolution of phases formed during the firing of the citrate precursor, in the thermal range 150–700 °C, was more deeply studied by XRD analysis. An amorphous material was identified after drying in vacuum oven. As may be seen in Fig. 2, low intensity peaks, assigned to poorly crystallized tetragonal $CuFe_2O_4$ oxide particles, were detected once the solid was calcined at 150 °C, by thermal decomposition of the citrate precursor. The markedly lower temperature of synthesis of $CuFe_2O_4$ powder, in comparison with the traditional procedure, is due to the intimate, atomic level mixing, of the constituent metals in the precursor.

The Bragg diffractions increased their intensities when temperature was raised, since the crystallinity of spinel phase was improved. The XRD pattern of the catalyst CIT700 clearly confirmed the presence of tetragonal $CuFe_2O_4$ spinel single phase, with the highest crystallinity. The unit cell dimensions

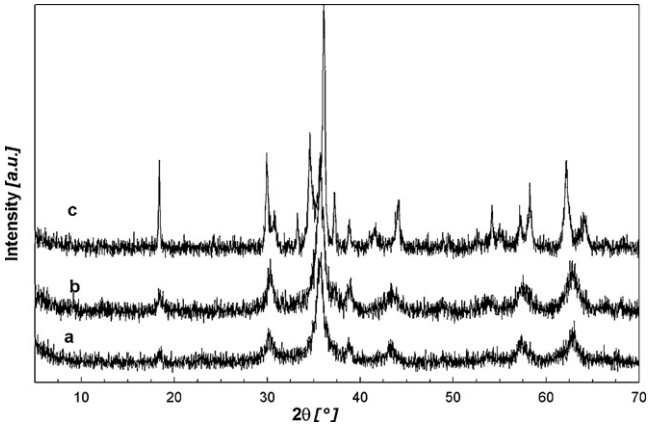

Fig. 2. XRD patterns of CIT catalysts, treated at different temperatures: (a) CIT150, (b) CIT400 and (c) CIT700.

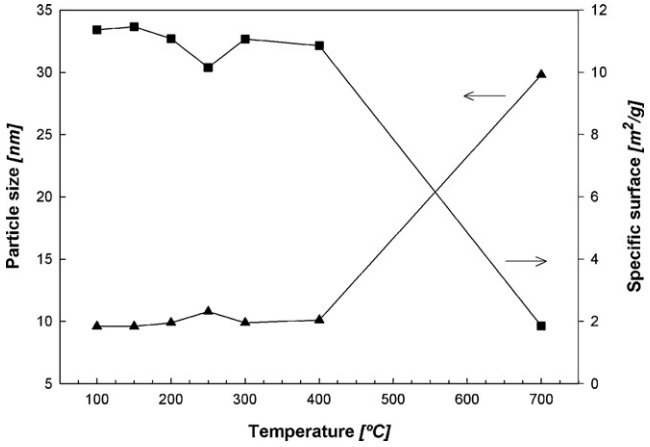

Fig. 3. Variation of grain sizes and specific surface areas with firing temperatures for CIT sample.

calculated were a: 8.205(3) Å and c: 8.725(3) Å, with c/a: 1.063, in accordance with the reported values [13,15,16].

A definite line broadening of the diffraction peaks observed in CIT150 is an indication that the synthesized materials are in the nanometer range. Subsequently a sharp increase in the crystalline nature of the copper ferrite powders was detected, as the firing temperature was increased, which is recorded as a decrease in the broadening of the peaks in the XRD pattern. This clearly indicates that the particle size increased with the increase of firing temperature. In order to get a deeper insight into the size particles distribution, during the thermal treatment of copper ferrite precursor, the evolution of size by the XRD data of the materials between 100 and 700 °C was analyzed. The crystallite sizes were estimated from the Debye–Scherrer formula applied to the major intensity peak (3 1 1) [17]. As can be seen from the plot shown in Fig. 3, it was found that the mean crystal size growths from 10 to 30 nm., in the thermal interval investigated. In addition to this, assuming all the particles to be spherical, the specific surface area of particles calculated decreases as the firing temperature rises.

3.2. IR characterization

The IR spectra of copper ferrites, obtained by SP and NIT chemical synthesis, at 950 and 700 °C, respectively, are identical. These show two strong bands at about 570 and 430 cm^{-1} which confidently can be assigned to the stretching vibration of the bonds Fe^{III}–O in tetrahedral and octahedral building units of inverted spinel, respectively [16].

The evolution of the FTIR spectra of the precursor and bulk catalysts obtained by CIT method thermally treated at 150, 400, and 700 °C were analyzed in order to determine the structural changes in the precursor during its decomposition. The spectrum of the solid coming from the vacuum oven was interpreted, taking into account the formation of a tridentate chelate complex with both, Fe^{3+} and Cu^{2+} cations. The infrared spectrum of the precursor is in agreement with other metallic citrate complexes spectra reported in the literature [18].

After the thermal treatment at 150 °C, the spectrum displays the disappearance of most absorptions belonging to the complex precursor. Furthermore, the most distinctive feature of the spectrum is that two new significant bands centered in ~600 and ~400 cm^{-1} appear at low energy. These intense absorptions are undoubtedly assigned to $CuFe_2O_4$ as the main pyrolysis product once the complex precursor is treated at 150 °C. These characteristic two band spectra, which belong to the pure spinel structure, are maintained in the solids calcined at 400 and 700 °C, in complete accordance with XRD data.

3.3. TGA/DTA of catalysts prepared by citrate route

According to this synthetic procedure, citric acid is not only a chelating agent but also a fuel. Therefore, the thermogram of the as-prepared precursor, extracted form the vacuum oven, was registered in order to study its thermal behavior at high temperature. Analyzing the TG curve, shown in Fig. 4, it can be observed that the decomposition of the precursor takes place in two thermal steps separated by a sharp signal around 150 °C. The smooth weight loss observed below 150 °C was attributed to water vaporization. This thermal accident is followed by a gradual decay of mass in the thermal range from 150 to 300 °C, which indicates that the decomposition reaction of the ferrite precursor has occurred. A similar effect has been reported for other spinel catalysts obtained by the citrate method [19]. Furthermore, these TG signals would correspond, according to the data obtained from DRX and FTIR measurements already discussed, to the thermal decomposition of the remainder citrate, still present in the material extracted from the vacuum oven, accompanied by the release of CO_2, H_2O, and NO_2 from the precursor. Consequently, after this step copper ferrite formation can be assured. This assignment is also supported by the similar results already reported for the related materials obtained from citrate precursor route [6,19,20].

From 300 °C to 700 °C, a slight mass loss is observed in the thermogram and no other thermal effects are observed in the formed phase, since the TG curve is almost featureless in the same range of temperatures.

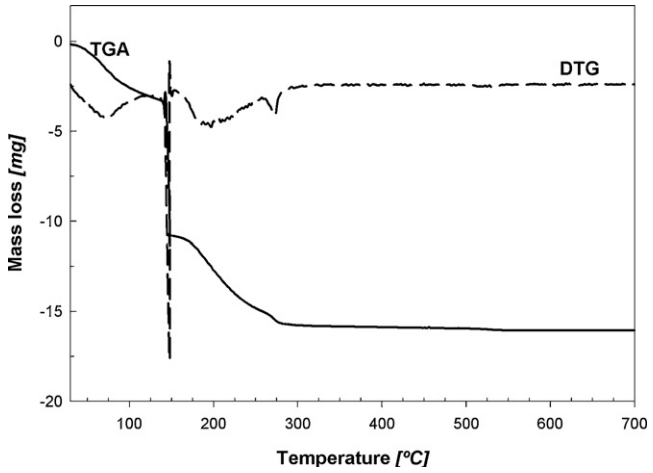

Fig. 4. TGA plot and DTG plot of the precursor prepared by CIT route.

3.4. Mössbauer characterization

The Mössbauer spectra of bulk catalysts were registered in order to analyze the Fe^{3+} cation distribution in the $CuFe_2O_4$ spinel lattice, with the synthetic procedures and also with their thermal treatment. The Mössbauer spectra, at room temperature, of SP, NIT, and CIT are displayed in Figs. 5a–c. On the other hand, Table 1 shows the corresponding fitting hyperfine parameters for each sample.

The Mössbauer spectra of bulk copper ferrite samples are composed of two magnetic sextets (MO and MT) with hyperfine fields (H) values detailed in Table 1, at RT; which were attributed to the Fe^{3+} cations located in octahedral (B sites) and tetrahedral (A sites) sublattices present in the spinel structure [8]. The distribution of cations in this type of structure may be described as $[Cu_{\delta x}Fe_{1-x}]^{A}[Cu_{1-\delta x}Fe_{1+x}]^{B}O_4$, being x the inversion parameter, whose value is among 0 and 1 for normal and inverse spinel, respectively.

The two sextets corresponding to $CuFe_2O_4$ are present in NIT and SP bulk catalysts and their spectral areas, representing 97% of total resonant signal, are assignable to spinel phases with different degrees of inversion as may be seen by the % spectral areas Mo and Mt, shown in Table 1. The remainder 3% of the total area is a paramagnetic doublet, assigned to Fe^{3+} according to the hyperfine parameters. This evidence would indicate the presence of some nanometric particles of $CuFe_2O_4$ with blocking temperature lower than RT, as already observed [15]. Regarding the Mössbauer spectrum of CIT bulk catalyst, it could be fitted similarly with the two magnetic sextets belonging to the two different Fe^{3+} sublattices. Consequently, it can be concluded that the synthesized $CuFe_2O_4$ phases belong to the inverse spinel structure, with different degrees of inversion dependent on the T and the synthetic procedure.

Table 1
Hyperfine parameters of bulk catalysts, by fitting the corresponding spectra at 298 K.

Catalysts	Parameters	M_O	M_T	P_1
SP950	$H(T)$	49.2	47.5	–
	δ (mm/s)	0.41	0.28	0.49
	2ε (mm/s)	−0.16	−0.01	–
	Δ (mm/s	–	–	1.52
	Γ (mm/s)	0.191	0.191	0.191
	A (%)	33.0	64.0	3.0
NIT700	$H(T)$	49.9	48.1	–
	δ (mm/s)	0.38	0.21	0.37
	2ε (mm/s)	−0.17	0.01	–
	Δ (mm/s	–	–	1.33
	Γ (mm/s)	0.147	0.147	0.147
	A (%)	46.2	51.4	2.4
CIT700	$H(T)$	51.4	47.7	
	δ (mm/s)	0.37	0.27	
	2ε (mm/s)	−0.10	−0.04	
	Δ (mm/s	–	–	
	Γ (mm/s)	0.240	0.240	
	A (%)	63.0	37.0	

References: (H) hyperfine magnetic field; (δ) isomer shift; (Δ) quadrupole splitting; (ε) quadrupole shift; (Γ) line width; (A) relative area.

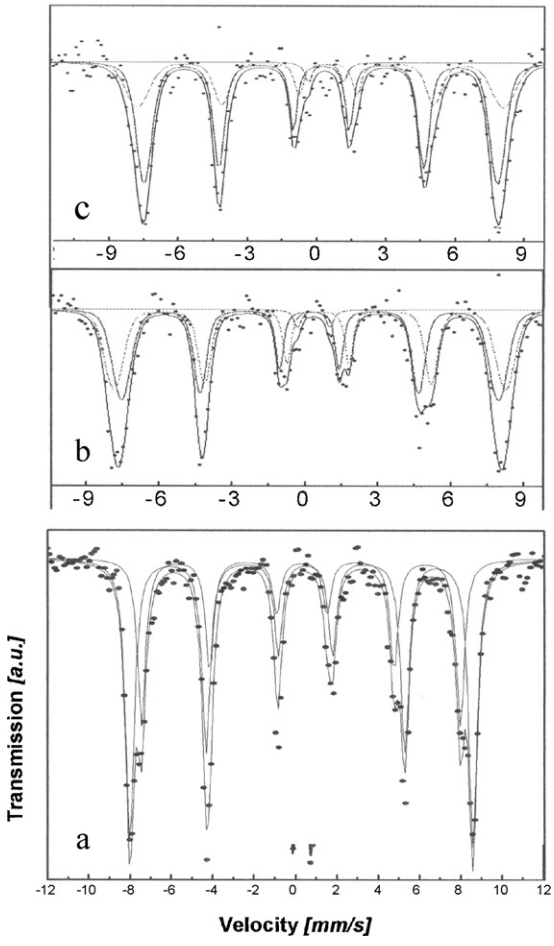

Fig. 5. Mössbauer spectra of the samples obtained by the different synthetic procedures: (a) CIT700, (b) NIT700 and (c) SP950.

Moreover, the higher value of hyperfine fields (H) was assigned to the Fe^{3+} in octahedral (B) sites whereas the lower value was related to Fe^{3+} in tetrahedral (A) sites, at RT. This assignment is due to the stronger hyperfine interaction A–O–B on the B sites and also to the lower covalency of the Fe^{3+}–$O^{=}$ bond in octahedral site [21].

From the comparison of the percentage of spectral areas belonging to Fe^{3+} ions in octahedral sites, it is observed that it increases as: SP950 < NIT700 < CIT700. This way, according to the Mössbauer spectra of the different samples, the Fe^{3+} cations are shifted from A-sites to B-sites, depending on the temperature and preparation routes applied. It is likely that NIT700 sample will show a similar occupation of Fe^{3+} in both octahedral and tetrahedral sites of spinel, whereas in the case of the samples SP950 and CIT700, other different distributions are achieved.

3.5. SEM-EDAX characterization

The morphology of CIT catalysts is influenced by the synthetic route. In the case of the material obtained by solid phase reaction SP950, the SEM image illustrated in Fig. 6a shows a homogenous microstructure consisting of dense rounded borders grains. This morphology should be attributed to the higher temperature of synthesis which allows the grain growth and a reduction of porosity.

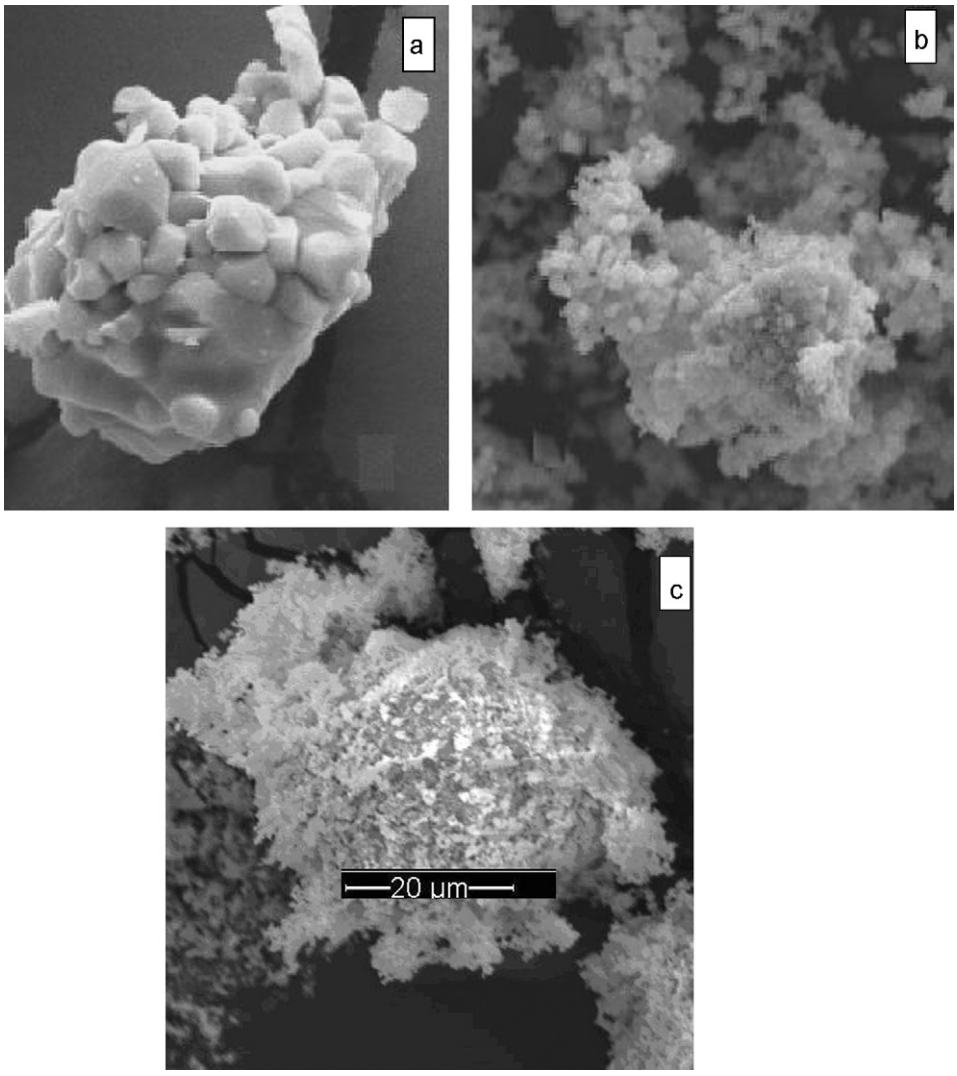

Fig. 6. SEM photographs of the catalysts: (a) SP950, (b) NIT700 and (c) CIT700.

According to Fig. 6b and c, it can be observed that the bulk catalysts obtained by wet chemical synthesis, at a lower temperature, i.e. NIT700 and CIT700, display irregular grains ranging from 1.2 to 2 μm with undefined edges, showing agglomeration to some extent. The observed shapes could be explained by the synthetic procedures applied, since the solids that have been formed departing from solutions. Therefore, the evaporation, followed by the pyrolysis of the precursor, yielded small particles of catalyst.

In order to get a deeper insight regarding the distribution of metallic cations on the surface of the catalyst CIT700, the EDAX scanning of the sample has been registered. As can be seen in Fig. 7b and c, it is possible to observe that, in the material obtained in mild conditions, the Cu and Fe are well dispersed on the grains surface, as well as that the Fe/Cu proportion equal to 2 was confirmed.

3.6. TEM analysis of ferrites obtained from CIT route

The morphology of ferrites obtained by citrate precursor during thermal treatment was investigated also by TEM. As showing in Fig. 8, the TEM images reveal the presence of nanoplatelets and nanoparticles showing a similar morphology to that of related ferrites, also obtained by soft chemistry procedures [7,22].

In order to determine the average size and the size distribution of particles, the analysis by counting particles on the TEM micrograph was carried out. The mean particle sizes were estimated from the TEM photographs according to the mean surface diameter [11]. The correlation with mean surface diameter is preferred because catalytic properties are directly related to surface area.

Fig. 9 shows the size particle distribution of CIT bulk catalyst, treated at 300 °C (a) and 700 °C (b), respectively. Evidently, the thermal treatment affects the particle size markedly. As can be seen in both figures, in the samples treated at 300 °C most of the particles are between 10 and 15 nm, in mean diameter. Whereas in the case of the materials calcined at 700 °C, most of the size distribution is below 60 nm, although a minor fraction reaches sizes of bigger magnitude and also some particles of over 200 nm were found. Thus, with the increase of calcination

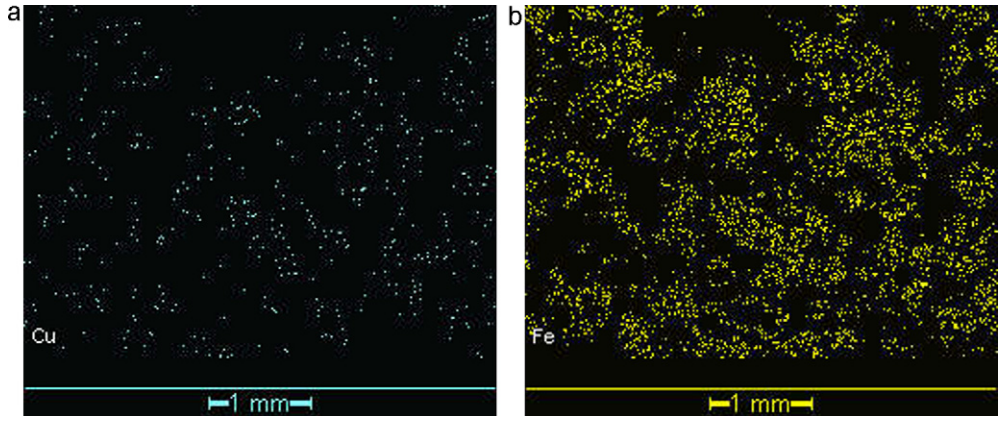

Fig. 7. EDAX scanning of CIT700 of Cu (a) and Fe (b).

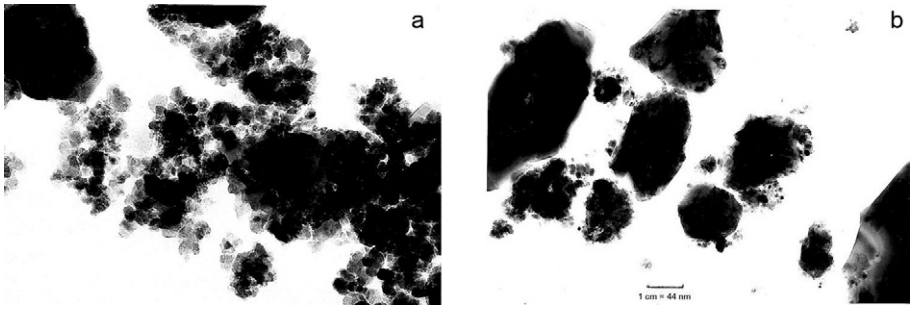

Fig. 8. TEM patterns of $CuFe_2O_4$ nanocrystals obtained by CIT procedure: (a) 300 °C and (b) 700 °C.

temperature the synthesized powders rapidly coarsen and become heterogeneous.

According to TEM data, the average particle sizes calculated are in good accordance with crystallite sizes, obtained by XRD measurement.

3.7. Textural properties

In order to analyze the temperature effect over the textural properties, specific surface (Sg) and pore volume (Vp), of catalysts prepared by wet chemical synthesis procedures were determined, as summarized in Table 2. It may be observed from data belonging to CIT samples that a significant surface area decrease was determined as a consequence of the thermal treatment. This effect should be attributed to the sintering of the active phase during the catalysts synthesis.

A similar trend was found for the specific surface values calculated from Debye–Scherrer equation. However the BET area determined for CIT700 is larger than that derived from the crystal size calculation due to the porosity of the material, resulting from the liberation of gasses from the precursor.

On the other hand, a slightly lower surface area is achieved in the case of the sample NIT700, in comparison with the related sample CIT700.

Table 2
BET textural properties of catalysts prepared by wet-chemical synthesis methods.

Samples	Sg ($m^2\ g^{-1}$)	Vp ($cm^3\ g^{-1}$)
CIT150	6.1	0.006
CIT400	6.4	0.007
CIT700	3.8	0.003
NIT700	2.7	0.005

3.8. Hydrogen TPR results

The H_2 TPR profiles of $CuFe_2O_4$, prepared by solid state and wet chemical reactions, were analyzed. The plot belonging to the catalyst NIT700 is depicted in Fig. 10, as a typical example. It was observed that all the samples exhibit two distinctive peaks. The first signal appearing in the thermal range 300–400 °C was assigned to the reduction of $CuFe_2O_4$ to metallic Cu and Fe_2O_3, and to the subsequent reduction of Fe_2O_3-hematite to Fe_3O_4-magnetite [23]. The peak appearing at high temperature, over 500 °C, is attributed to the reduction of Fe_3O_4 to FeO, followed by the reduction to metallic Fe. These results are in accordance with previously reported assignments [23,24].

According to the data obtained, the temperatures of reduction are identical for SP950 and NIT700 whereas in the case of the sample labeled CIT700, the first peak is shifted towards lower temperature, at 320 °C, and the second is observed at higher temperature, around 750 °C, with some degree of splitting. Hence, the temperature difference between the first and last peak in the latter is the highest, suggesting that a more efficient redox system for electron transfer would be achieved in this material.

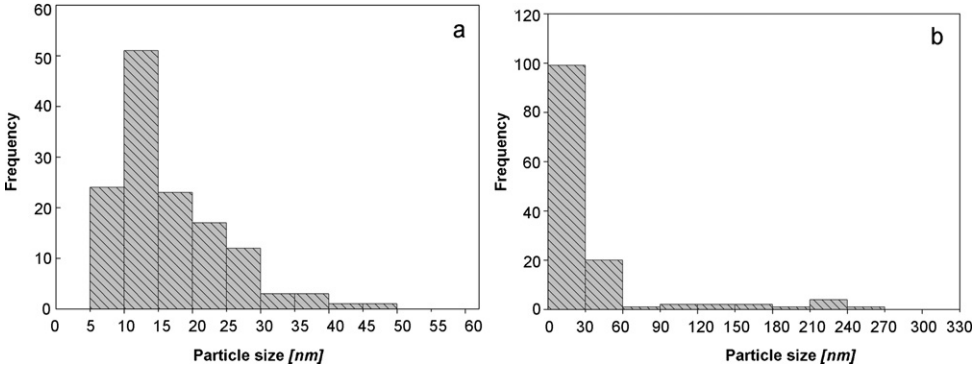

Fig. 9. Particle size distribution of CIT catalysts: (a) treated at 300 °C and (b) treated at 700 °C.

3.9. Catalytic activity

Propane combustion was chosen as test reaction in order to study the catalytic behavior of the materials prepared by the three different preparation routes. Fig. 11 shows the influence of temperature on the propane combustion measured over the bulk catalysts. As may be seen the propane conversion over sample SP950 increases by increasing the reaction temperature to reach a maximum value of ca. 100% around 750 °C. Conversely, the catalyst NIT700 and CIT700 prepared by wet chemical procedures, annealed at identically lower temperature, display improved catalytic activity since their conversion profiles are shifted to lower temperature reaching total conversion at around 650 °C. The appearance of CO was not observed in any of the experiments.

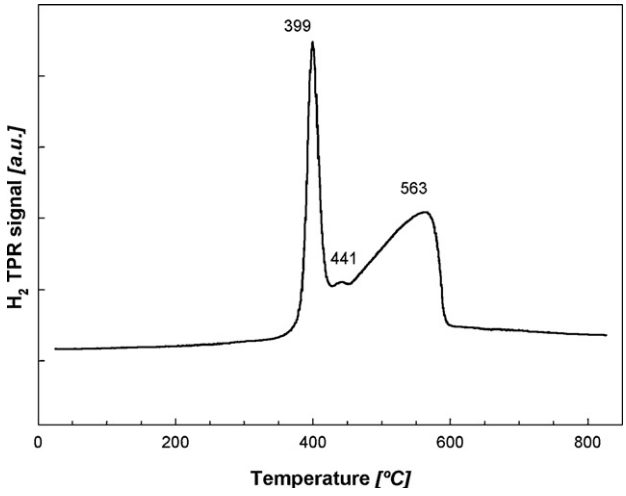

Fig. 10. TPR curve for NIT700 catalyst.

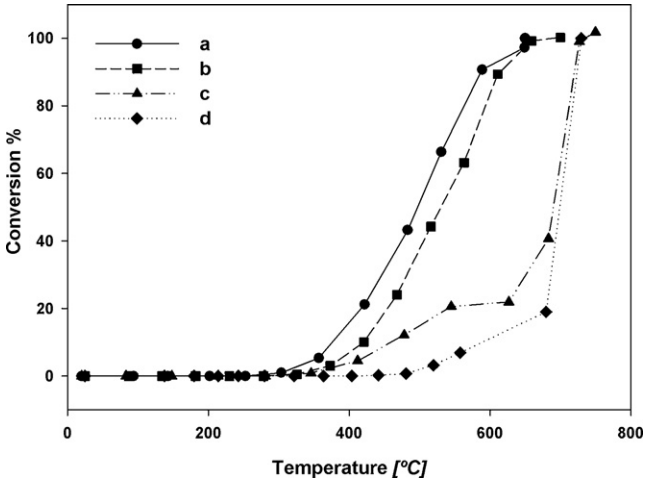

Fig. 11. Light-off plots for propane combustion of catalysts prepared by the different routes: (a) NIT700, (b) CIT7000, (c) SP950 and (d) in absence of catalyst.

For comparison the combustion curve for the homogeneous process, in absence of catalyst, is superimposed to the rest of the experiments. As can be seen it shows a displacement to higher temperature, in comparison with the heterogeneous process, as expected.

To quantitatively compare the catalysts activities, Table 3 shows the temperature values to reach 50% (T50) and 90% (T90) propane conversion to CO_2 and H_2O, respectively.

According to these conversion data, the spinel $CuFe_2O_4$ behaves as an active catalyst for propane combustion, displaying differences depending on the chemical synthesis. As discussed in the previous paragraph, the synthetic procedure has influence on the crystal structure, cation distribution in the spinel sites, morphology, active surface, and therefore on the catalytic activity.

Comparing the synthetic methods, it is worthwhile noticing that the sample SP950, annealed at higher temperature, which is characterized by cubic spinel structure, partially inverse, according to Mössbauer spectra, and a coarse sintered microstructure; exhibited lower capability as HC catalyst. Indeed, at around 540 °C the slope of the curve dramatically changes, keeping almost constant between 540 °C and 630 °C; and then increases steadily up to 750 °C. Moreover, it locates close to the plot of the homogeneous process and therefore this behavior suggests that the deactivation of this catalyst would have occurred.

On the other hand, in the samples obtained in mild conditions, these are more catalytically active. In the case of

Table 3
T_{50} and T_{90} values for propane combustion.

Samples	T_{50}	T_{90}
SP950	680	720
NIT700	448	520
CIT700	530	619

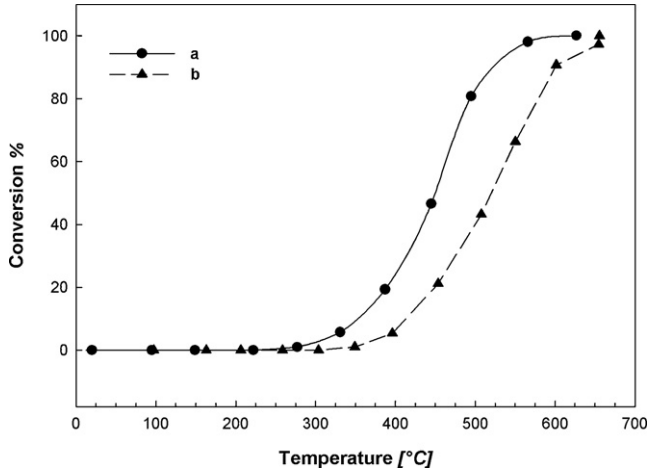

Fig. 12. Light-off plots for propane combustion of NIT700: (a) in presence of NO and (b) in absence of NO.

NIT700 and CIT700 materials, the lower temperature of annealing assures the presence of tetragonal spinel cell with high BET surface, surely due to the presence of small size particle and also to the irregular morphology, observed by SEM.

Furthermore, in the case of the material labeled CIT700 the main physicochemical parameters measured are favorable for catalytic activity. In fact, the presence of nanometric particles was confirmed by TEM analysis, specific surface was the highest and an efficient redox behavior was measured.

However, the efficiency for HC conversion is somehow lower for CIT700 than for NIT700. In order to find a possible explanation to this behavior, the comparison of the distribution of cation in the sublattices in spinel for both NIT700 and CIT700 materials was carried out.

Based on the Mössbauer data obtained, it is observable that in NIT700 the cation Fe^{3+} is occupying, in almost the same proportion, the tetrahedral and octahedral sites of typically inverted spinel structure. Meanwhile, a higher occupation with Fe^{3+} of octahedral sites is observed in CIT700 indicating that a partially inverted spinel was achieved.

It seems that the typically inverted spinel structure of NIT700 would favor the availability of catalytic sites in this material.

The propane oxidation on NIT700 sample was also analyzed in presence of NO traces. This reaction is of interest since NO is the habitual pollutant in the exhaust of combustion processes. According to this, 1000 ppm NO was added to the feed. A shift towards a lower temperature is observed, as shown in Fig. 12. This behavior suggests that the activation of this catalyst is modified by the presence of NO. It is likely that the enhancement in the catalytic performance could be attributed to more highly NO_2 oxidant than oxygen.

4. Conclusions

The obtained results allow us to conclude that the copper ferrites obtained at 700 °C, using nitrate and citrate routes; seem to be more active catalysts for the propane combustion than the material obtained by traditional ceramic procedure. The most relevant properties for the catalytic performance of HC combustion seem to be: the presence of small particles of inverted spinel $CuFe_2O_4$ in the nanometric scale, with irregular morphology, high specific surface, and the convenient reducibility behavior. In addition to this, the typically inverted spinel structure found in NIT700 would favor the availability of catalytic sites in this material.

Acknowledgements

The authors would like to acknowledge the economic support for this work to the UNLP, UNCPBA, ANPCYT and CONICET, Argentina and to Lic. M.E. Canafoglia for her collaboration with SEM-EDAX measurements.

References

[1] T.V. Choudhary, S. Banerjee, V.R. Choudhary, Catalysts for combustion of methane and lower alkanes, Appl. Catal. A 234 (2002) 1–23.
[2] S. Kameoka, T. Tanabe, A.P. Tsai, Spinel $CuFe_2O_4$: a precursor for copper catalyst with high thermal stability and activity, Catal. Lett. 100 (2005) 89–93.
[3] M. Alifanti, N. Blangenois, M. Florea, B. Demon, Supported Co-based perovskites as catalysts for total oxidation of methane, Appl. Catal. A 280 (2005) 255–265.
[4] Y. Teraoka, K. Nakano, W. Shangguan, S. Kagawa, Simultaneous catalytic removal of nitrogen oxides and diesel soot particulate over perovskite-related oxides, Catal. Today 27 (1996) 107–113.
[5] J. Kircherova, M. Alifanti, B. Delmon, Evidence of phase cooperation in the $LaCoO_3$–CeO_2–Co_3O_4 catalytic system in relation to activity in methane combustion, Appl. Catal. 231 (2002) 65–80.
[6] Y. Huang, Y. Tang, J. Wang, Q. Chen, Synthesis of $MgFe_2O_4$ nanocrystallites under mild conditions, Mater. Chem. Phys. 97 (2006) 394–397.
[7] S. Arnone, G. Bagnasco, G. Busca, L. Lisis, G. Russo, M. Turco, Catalytic combustion of methane over transition metal oxides, Stud. Surf. Sci. Catal. 119 (1998) 65–70.
[8] Q. Liu, L. Wang, M. Chen, Y. Cao, H. He, K. Fan, Dry citrate-precursor synthesized nanocrystalline cobalt oxide as highly active catalyst for total oxidation of propane, J. Catal. 263 (2009) 104–113.
[9] G. Pantaleo, L.F. Liotta, A.M. Venezia, G. Deganello, E.M. Ezzo, M.A. ElKherbawi, H. Atia, Support effect on the structure and CO oxidation activity of Cu–Cr mixed oxides over Al_2O_3 and SiO_2, Mater. Chem. Phys. 114 (2009) 604–611.
[10] T. Liu, L. Wang, P. Yang, B. Hu, Preparation of nanometer $CuFe_2O_4$ by auto-combustion and its catalytic activity on the thermal decomposition of ammonium perchlorate, Mater. Lett. 62 (2008) 4056–4058.
[11] A.F. Wells, Química Inorgánica Estructural, Ed. Reverté, Barcelona, 1978 (Chapter 12).
[12] P. Gallezot, C. Leclerc, in: B. Imelick, J.C. Vedrine (Eds.), Catalyst Characterization, Plenum Press, New York, 1994, p. p. 537.
[13] M. Ristić, B. Hannoyer, S. Popović, S. Musić, N. Bajraktaraj, Ferritization of copper ions in the Cu–Fe–O system, Mater. Sci. Eng. B77 (2000) 73–82.
[14] X. Tang, A. Manthiram, J.B. Goodenough, Copper ferrite revisited, J. Solid State Chem. 79 (1989) 250–262.
[15] G.F. Goya, H.R. Rechenberg, J.Z. Jiang, Structural and magnetic properties of ball milled copper ferrite, J. Appl. Phys. 84 (1998) 1101–1108.
[16] R. Kalai Selvan, C.O. Augustin, L. John Berchmans, R. Saraswathi, Combustion synthesis of $CuFe_2O_4$, Mater. Res. Bull. 38 (2003) 41–54.
[17] M. George, A.M. John, S.S. Nair, P.A. Joy, M.R. Anantharaman, Finite size effects on the structural and magnetic properties of sol–gel synthesized $NiFe_2O_4$ powders, J. Magn. Magn. Mater. 302 (2006) 190–195.

[18] N.B. Lin-Vien, W.G. Colthup, J. Fateley, D. Grasselli, The Handbook of Infrared and Raman Frequencies of Organic Molecules, Academic Press, Boston, 1991.
[19] Z. Yue, W. Gou, J. Zhou, Z. Gui, L. Li, J. Magn. Magn. Mater. 270 (2004) 216–223.
[20] M.N. Barroso, M.F. Gómez, J. Andrade Gamboa, L.A. Arrúa, M.C. Abello, J. Phys. Chem. Solids 67 (2006) 1583–1589.
[21] R. Kalai Selvan, C.O. Augustin, M.I. Oshtrakh, O.B. Miller, V.A. Semionkin, Mössbauer and D.C. magnetization studies of $(CuFe_2O_4)_{1-x}(SnO_2)_x$ (x = 0 and 5 wt%) nanocomposites, Hyperf. Inter. 165 (2005) 231–237.
[22] Q. Liu, J. Sun, H. Long, X. Sun, X. Zhong, Z. Xu, Hydrothermal synthesis of $CoFe_2O_4$ nanoplatelets and nanoparticles, Mat. Chem. Phys. 108 (2008) 269–273.
[23] K. Faungnawakij, R. Kikuchi, T. Fukunaga, K. Eguchi, Catalytic hydrogen production from dimethyl ether over $CuFe_2O_4$ spinel-based composites: hydrogen reduction and metal dopant effects, Catal. Today 138 (2008) 157–161.
[24] W. Curtis Conner Jr., G.M. Pajonk, S.J. Teichner, Spillover of sorbed species, Adv. Catal. 34 (1986) 1–79.